# Supplementary Material

# Competition between water uptake and ice nucleation by glassy organic aerosol particles

T. Berkemeier[1,2,*], M. Shiraiwa[1], U. Pöschl[1] and T. Koop[2,*]

[1] Multiphase Chemistry Department, Max Planck Institute for Chemistry, Mainz, Germany

[2] Faculty of Chemistry, Bielefeld University, Bielefeld, Germany

Correspondence to: T. Berkemeier (t.berkemeier@mpic.de), T. Koop (thomas.koop@uni-bielefeld.de)

## 1. Treatment of gas diffusion

To account for local depletion of trace gases in the near-surface gas phase of aerosol particles acting as a sink for the respective gases, Shiraiwa et al. (2012) use a gas phase diffusion correction factor for species Z, $C_{g,Z}$, as described previously by Pöschl et al. (2007). In this formalism a corrected near-surface trace gas concentration $[Z]_{gs}$ is obtained through the uptake coefficient of Z, $\gamma_Z$, and the Knudsen number $Kn_Z$ of the diffusion system. Since the trace gas uptake $\gamma_Z$ itself depends on $[Z]_{gs}$ and thus via $C_{g,Z}$ on its own value, this formalism significantly increases the stiffness of the set of differential equations that needs to be solved. In the new formalism, a different approach of gas phase diffusion correction is employed. The approach assumes a gaseous shell with a thickness of one mean free path $\lambda_Z$ around the particle as well, but treats all mass fluxes to and from this shell explicitly in a separate differential equation. In particular, the diffusion flow $F_{net,Z}$ from this far-surface gas phase into the near-surface gas shell can be calculated as diffusion through a virtual particle envelope with $d_p + 2\,\lambda_Z$ diameter (Pöschl et al., 2007). Applying Fick's first law yields

$$\boldsymbol{F_{net,g,Z} = 4\pi(r_p + \lambda_Z)D_{g,Z}([Z]_g - [Z]_{gs})}. \qquad \text{(S1)}$$

Since in all calculations that we performed, particle size was approximately on the order of the mean free path, we chose the respective limiting case for calculation of the mean free path

$\boldsymbol{\lambda_Z}$ differently from Pöschl et al. (2007) by using Eq. (S2) as given in Seinfeld and Pandis (2006) and valid for $d_p \approx \lambda_Z$.

$$\boldsymbol{\lambda_Z = \frac{1.7\, D_{g,Z}}{\omega_Z}} \tag{S2}$$

## 2. Physico-chemical parameterizations

In the following sections we list all physico-chemical parameterizations employed in this study. For simulations of the sucrose/water model system, we use parameterizations for density, water activity and bulk diffusivity by Zobrist et al. (2011). Glass transition values are taken from Zobrist et al. (2008), gas diffusivities of water from Winkler et al. (2006), while vapor pressures of ice and water are taken from Murphy and Koop (2005). A few miscellaneous model parameters are compiled in Table S3.

### *2.1. Density*

For the sucrose/water system density can be parameterized as a function of the organic weight fraction $w_{org}$ with a fourth-order polynomial function (Zobrist et al., 2011).

$$\boldsymbol{\rho_{tot}(w_{org}) = a_0 + a_1 w_{org} + a_2 w_{org}^2 + a_3 w_{org}^3 + a_4 w_{org}^4} \tag{S3}$$

where $\boldsymbol{a_0 = 0.9989}$, $\boldsymbol{a_1 = 0.3615}$, $\boldsymbol{a_2 = 0.2964}$, $\boldsymbol{a_3 = -0.3186}$ and $\boldsymbol{a_4 = 0.24191}$.

For all other systems, volume additivity was assumed, leading to the following expression of density as function of $w_{org}$ and density $\rho_{org}$ of the pure compounds.

$$\boldsymbol{\rho_{tot}(w_{org}) = \frac{1}{(1 - w_{org}) + \frac{w_{org}}{\rho_{org}}}} \tag{S4}$$

### *2.2. Water activity*

For the determination of water activity from composition data, several different approaches are used. For sucrose and levoglucosan, parameterizations from Zobrist et al. (2011) and Zobrist et al. (2008) are used, respectively. In these parameterizations, water activity is described as function of temperature and organic weight fraction as follows:

$$a_{\mathrm{w}}(T, w_{\mathrm{org}}) = \frac{1 + a w_{\mathrm{org}}}{1 + b w_{\mathrm{org}} + c w_{\mathrm{org}}^2} + (T - T^{\ominus})(d w_{\mathrm{org}} + e w_{\mathrm{org}}^2 + f w_{\mathrm{org}}^3 + g w_{\mathrm{org}}^4) \tag{S5}$$

Parameters for these two substances are given in Table S4. For substances for which no previous parameterization was available, we employ Kappa-Koehler theory, using the single hygroscopicity parameter $\kappa_{\mathrm{org}}$ or the equivalent van't Hoff parameter $i_{\mathrm{org}}$ to determine water activity (Petters and Kreidenweis, 2007).

$$a_{\mathrm{w}}(w_{\mathrm{org}}) = \frac{1}{1 + \frac{\kappa_{\mathrm{org}}}{p_{\mathrm{org}}} \cdot \frac{w_{\mathrm{org}}}{1 - w_{\mathrm{org}}}} = \frac{1}{1 + i_{\mathrm{org}} \cdot \frac{M_{\mathrm{w}}}{M_{\mathrm{org}}} \frac{w_{\mathrm{org}}}{1 - w_{\mathrm{org}}}} \tag{S6}$$

For citric acid, a composition-dependent fit of $i_{\mathrm{org}}$ has been provided by Koop et al. (2011).

$$i_{\mathrm{org}} = 1 + 2.1408 w_{\mathrm{org}}^2 \tag{S7}$$

Lienhard et al. (2012) give an alternative parameterization that behaves differently especially at lower temperatures (cf. Figure B2). We note however that at T < 220 K we use the parameterization outside of its validity range. The functional form of this parameterization is given in Eq. (S8) and parameters given in Table S5.

$$\begin{aligned} a_{\mathrm{w}} &= \frac{1 - w_{\mathrm{org}}}{1 + q \cdot w_{\mathrm{org}} + r \cdot w_{\mathrm{org}}^2} \\ q &= a_1 + a_2 T + a_3 T^2 \\ r &= a_4 + a_5 T + a_6 T^2 \end{aligned} \tag{S8}$$

### *2.3. Bulk diffusivity*

Bulk diffusivity of water in the aqueous organic mixtures, $D_{\mathrm{H2O}}$, is parameterized using a (modified) Vogel-Fulcher-Tammann (VFT) approach that uses three parameters to account for its super-Arrhenius dependence on temperature (Vogel, 1921;Fulcher, 1925;Tammann and Hesse, 1926).

$$D_{\mathrm{H2O}}(T, a_{\mathrm{w}}) = 10^{-\left(A(a_{\mathrm{w}}) + \frac{B(a_{\mathrm{w}})}{T - T_0(a_{\mathrm{w}})}\right)} \tag{S9}$$

Here, $T_0$ is the so-called Vogel temperature, indicating the temperature at which $D_{\mathrm{H2O}}$ goes to zero. $T_0$ is closely related to the Kauzmann temperature, $T_{\mathrm{k}}$, that is the hypothetical point where the entropy of amorphous and crystalline solid would coincide, which is often referred to as the "Kauzmann paradox" (Kauzmann, 1948;Stillinger, 1988). Parameter $A$ can be

regarded as the high temperature maximum of water diffusivity ($T >> T_0$), whereas $B$ represents the steepness of the viscous slowdown, the so-called *fragility* (Angell, 1985, 1995). According to Angell (1985), a liquid with low $B$ exhibits *fragile* character, indicating a strong deviation of the temperature dependence from Arrhenius behaviour. Liquids with high $B$ on the other hand (e.g. network formers such as $SiO_2$) show the typical Arrhenius behaviour and are classified as *strong* liquids.

Zobrist et al. (2011) provided a set of water activity-dependent fit functions for the sucrose/water system based on experimental data over a wide temperature and concentration range.

$$\boldsymbol{A(a_{\mathrm{w}}) = 7 + 0.175\left(1 - 46.46(1 - a_{\mathrm{w}})\right)} \tag{S10}$$

$$\boldsymbol{B(a_{\mathrm{w}}) = 262.867(1 + 10.53(1 - a_{\mathrm{w}}) - 0.3(1 - a_{\mathrm{w}})^2)} \tag{S11}$$

$$\boldsymbol{T_0(a_{\mathrm{w}}) = 127.9(1 + 0.4514(1 - a_{\mathrm{w}}) - 0.5(1 - a_{\mathrm{w}})^{1.7})}. \tag{S12}$$

### *2.4. Glass transition*

In a binary system glass transition temperatures of mixtures can be described as a function of $w_{\mathrm{org}}$ by the Gordon-Taylor equation (Gordon and Taylor, 1952), using the glass transition temperature of the pure components ($T_{\mathrm{g,H2O}}$ and $T_{\mathrm{g,org}}$) and the Gordon-Taylor coefficient $k_{\mathrm{GT}}$:

$$\boldsymbol{T_{\mathrm{g}}(w_{\mathrm{org}}) = \frac{(1 - w_{\mathrm{org}})\, T_{\mathrm{g,w}} + \frac{1}{k_{\mathrm{GT}}} w_{\mathrm{org}} T_{\mathrm{g,org}}}{(1 - w_{\mathrm{org}}) + \frac{1}{k_{\mathrm{GT}}} w_{\mathrm{org}}}} \tag{S13}$$

The component with the lower glass transition temperature, in this case water, acts as a plasticizer, decreasing the glass point of the mixture with decreasing weight fraction $w_{\mathrm{org}}$.

### *2.5. Gas phase diffusivity*

The gas phase diffusion coefficient of water can be obtained using the temperature and pressure dependent parameterization provided in Winkler et al. (2006),

$$\boldsymbol{D_{\mathrm{g,H2O}}(T, p) = 1.9545\, T^{1.6658}\, p^{-1}}. \tag{S14}$$

### *2.6. Vapor pressures of ice and water*

Above 110 K, the vapor pressure of hexagonal ice is parameterized according to Murphy and Koop (2005) as

$$p_{\mathrm{ice}}(T) = \exp\left(9.550426 - \frac{5723.265}{T} + 3.53068 \ln T - 0.00728332\, T\right). \tag{S15}$$

For the vapor pressure of water, Murphy and Koop provided

$$\ln p_{\mathrm{liq}}(T) = 54.842763 - \frac{6763.22}{T} - 4.210 \ln T + 0.000367\, T + \tanh[0.0415(T - 218.8)]\left(53.878 - \frac{1331.22}{T} - 9.44523 \ln T + 0.014025\, T\right) \tag{S16}$$

for temperatures between 123 K and 332 K. Both parameterizations have been used in this study.

## Supporting Tables

Table S1. SOA marker substances used to estimate water diffusivities and estimated melting point and glass transition values.

| Name | Structure | *M* (g mol-1) | $T_m$, est./(lit.) (K) | $T_g$, est. (K) |
|---|---|---|---|---|
| **A-PINENE** | | | | |
| C107OOH† | 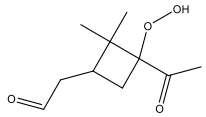 | 200.231 | 320.01 | 224.01 |
| PINONIC† / pinonic acid | 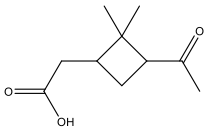 | 184.232 | 349.60 (378.65) | 244.72 |
| C97OOH† | 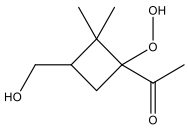 | 188.221 | 346.31 | 242.41 |
| C108OOH† | 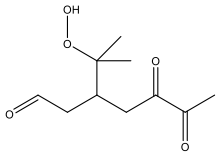 | 216.231 | 323.83 | 226.68 |
| C89CO2H† | 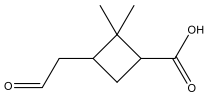 | 170.206 | 348.78 | 244.15 |
| PINIC‡ / pinic acid | 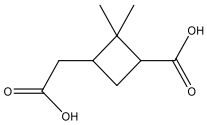 | 186.205 | 420.30 (355) | 294.21 |
| C921OOH† | 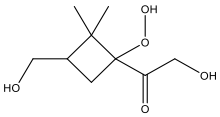 | 204.220 | 367.19 | 257.03 |
| C109OOH† | 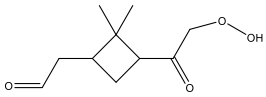 | 200.231 | 298.17 | 208.72 |
| C812OOH† | 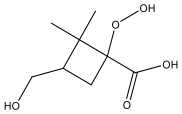 | 190.194 | 441.53 | 309.07 |

| | | | | |
|---|---|---|---|---|
| HOPINONIC† | 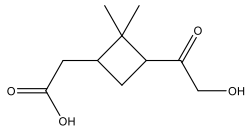 | 200.232 | 371.25 | 259.88 |
| C811OH† | 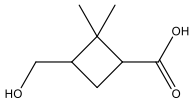 | 158.094 | 380.32 | 266.22 |
| C813OOH† | 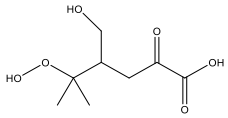 | 206.193 | 548.31 | 383.81 |
| ALDOL_dimer‡ | 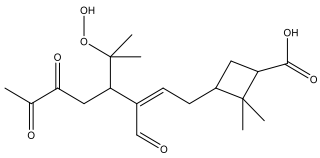 | 368.421 | 391.59 | 274.11 |
| ESTER_dimer‡ | 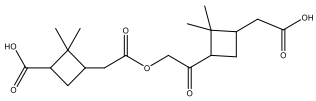 | 368.421 | 424.07 | 296.85 |
| pinonaldehyde | 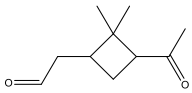 | 168.23 | 278.08 | 194.65 |
| terpenylic acid | 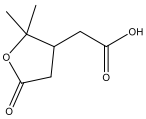 | 172,17 | 433.1 | 303.66 |
| 2-hydroxy terpenylic acid | 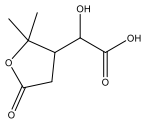 | 188,17 | 524.57 | 367.20 |
| diaterpenylic acid acetate | 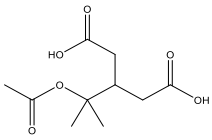 | 232,22 | 391.86 | 274.31 |
| 3-MBCTA | 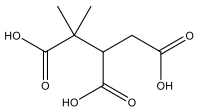 | 204.177 | 480.26 | 336.18 |
| **ISOPRENE** | | | | |
| $C_5$ alkene triol (aldol form) | 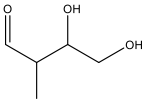 | 118.127 | 304.68 | 213.28 |
| $C_5$ alkene triol (keto form) | 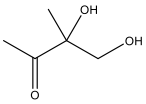 | 118.127 | 346.16 | 242.31 |

| | | | | |
|---|---|---|---|---|
| 2-methyltetrol | 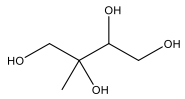 | 136.142 | 404.73 | 283.31 |
| $C_5$ trihydroxy acid | 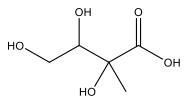 | 150.125 | 441.04 | 308.73 |
| hemiacetal dimer | 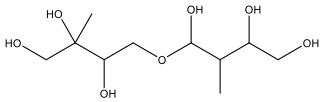 | 254.269 | 407.63 | 285.34 |
| methyltetrol performate | 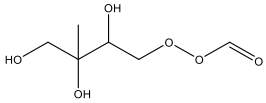 | 180.15 | 393.30 | 275.31 |
| 2-methylglyceric acid | 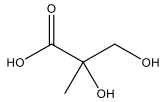 | 120.1 | 416.87 | 291.81 |
| 2-MG/mono- acetate dimer | 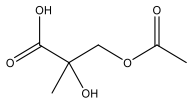 | 162.14 | 381.46 | 267.02 |
| 2-MG/2-MG dimer | 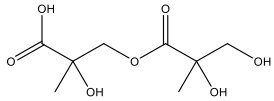 | 222.185 | 475.66 | 332.96 |
| $(2\text{-MG})_3$ trimer | 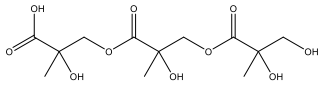 | 324.27 | 500.75 | 350.52 |
| $(2\text{-MG})_4$ tetramer | … | 426.355 | 516.47 | 361.53 |
| **NAPHTHALENE** | | | | |
| Kautzman122$^{\$}$/ benzoic acid | 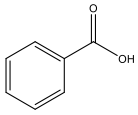 | 122.116 | 384.80 (395.5) | 269.36$^{*}$ |
| Kautzman138$^{\$}$ | 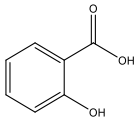 | 138.115 | 459.00 (431.75) | 321.30$^{*}$ |
| Kautzman166$^{\$}$ / phthalic acid | 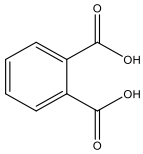 | 166.124 | 538.92 (403.15 decomp.) | 377.25$^{*}$ |
| 1-Hydroxy-naphthalene | 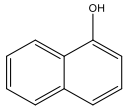 | 144.170 | 362.87 (368.15) | 257.71$^{*}$ |

| | | | | |
|---|---|---|---|---|
| 2-Hydroxy-naphthalene | 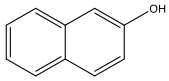 | 144.170 | 362.87 (394.65) | 276.26* |
| 1,2-naphthalene-dione | 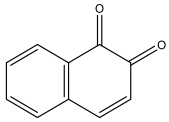 | 158.154 | 457.35 (419.15) | 293.41* |
| 1,4-naphthalene-dione | 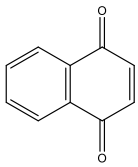 | 158.154 | 457.35 (401.65) | 281.16* |
| 2-Hydroxy-1,4-naphthalenedione | 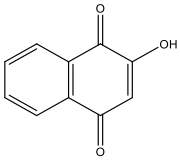 | 174.153 | 533.47 (468) | 327.60* |
| 5-Hydroxy-1,4-naphthalenedione | 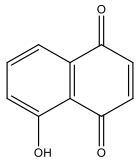 | 174.153 | 396.32 (428) | 299.60* |
| Kautzman192$ / 2-carboxy-cinnamic acid | 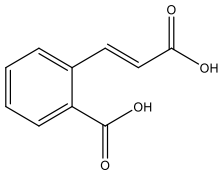 | 192.171 | 561.06 (473.15) | 331.21* |
| **DODECANE** | | | | |
| CARB§ | 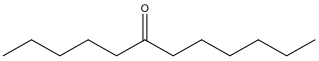 | 184.31 | 272.12 | 190.48 |
| THF derivative | 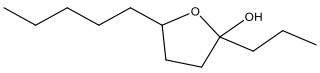 | 200.31 | 368.27 | 257.79 |
| CARBROOH§ | 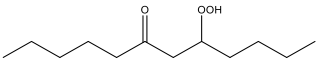 | 216.31 | 311.74 | 218.22 |
| OHDICARB§ | 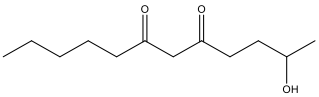 | 214.29 | 284.36 | 199.05 |
| Peroxydiol1 | 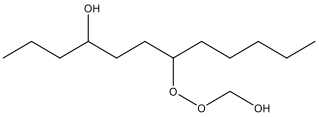 | 248.35 | 307.59 | 215.31 |
| Peroxydiol2 | 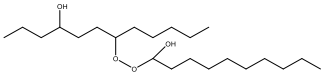 | 374.58 | 326.45 | 228.51 |

| | | | | |
|---|---|---|---|---|
| Peroxyketone1 | 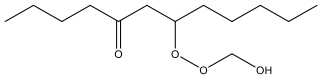 | 246.33 | 285.74 | 200.02 |
| Peroxyketone2 | 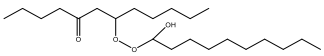 | 386.59 | 329.43 | 230.60 |
| OHCARBROOH[§] | 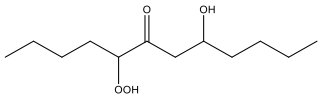 | 232.31 | 314.74 | 220.32 |
| CnACID C7H14O3[§] | 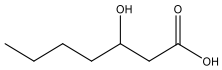 | 146.18 | 328.47 | 229.93 |
| Zhang299[¶] | 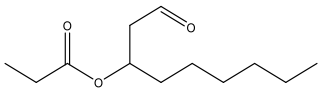 | 214.29 | 270.86 | 189.60 |
| Zhang301[¶] | 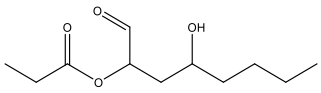 | 216.27 | 296.82 | 207.77 |
| Zhang315[¶] | 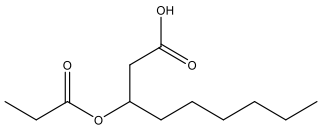 | 230.29 | 308.34 | 215.84 |

[*]: Glass transition temperature estimated from literature melting point.
[†]: Compound name adopted from MCM (master chemical mechanism).
[‡]: Compound name adopted from Zuend and Seinfeld (2012).
[$]: Compound name refers to MS peak with according m/z in Kautzman et al. (2010).
[§]: Compound name adopted from Yee et al. (2012).
[¶]: Compound name refers to MS peak with according m/z in Zhang et al. (2014).

Table S2. Full list of upper temperature limits (in K) for heterogeneous ice nucleation.

| **SOA Class** | **O/C** | **Lower estimate** | **Best guess** | **Upper estimate** |
|---|---|---|---|---|
| A-PINENE | 0.3 | 207.48 | 212.56 | 217.69 |
| | 0.5 | 213.20 | 217.46 | 221.88 |
| | 0.7 | 215.80 | 220.90 | 225.96 |
| ISOPRENE | 0.6 | 202.43 | 210.67 | 218.73 |
| | 0.8 | 206.21 | 211.99 | 218.10 |
| | 1.0 | 206.28 | 213.28 | 220.38 |
| NAPHTHALENE | 0.3 | 223.06 | 226.06 | 229.09 |
| | 0.5 | 219.21 | 223.27 | 227.37 |
| | 0.7 | 216.08 | 221.46 | 226,72 |
| DODECANE | 0.1 | 211.79 | 215.73 | 219.55 |
| | 0.3 | 205.69 | 209.29 | 213.15 |
| | 0.5 | 199.12 | 204.92 | 211.10 |

Table S3. Various model parameters.

| $T_{g,H2O}$ (K) | $\alpha_{s,0}$ () | $\tau_{D,H2O}$ (s) | $\rho_{org}$ (g cm$^{-3}$) | $M_{org}$ (g mol$^{-1}$) |
|---|---|---|---|---|
| 136 | 1 | 4e-11 | 1.4 | 250 |

Table S4. Parameters for water activity parameterization, Eq. (S5).

| Substance | a | b | c | d | e | f | g |
|---|---|---|---|---|---|---|---|
| Sucrose | –1 | –0.99721 | 0.13599 | 0.001688 | –0.005151 | 0.009607 | –0.006142 |
| Levoglucosan | –0.99918 | –0.90978 | 0.021448 | 0.00045933 | 0.0035813 | 0.00026549 | 0.0033059 |

Table S5. Parameters for water activity parameterization, Eq. (S8), after Lienhard et al. (2012).

| Substance | $a_1$ | $a_2$ | $a_3$ | $a_4$ | $a_5$ | $a_6$ |
|---|---|---|---|---|---|---|
| Citric acid | −3.16761 | 0.01939 | −4.02725e-5 | 6.59108 | −0.05294 | 1.06028e−4 |

## Supporting Figures

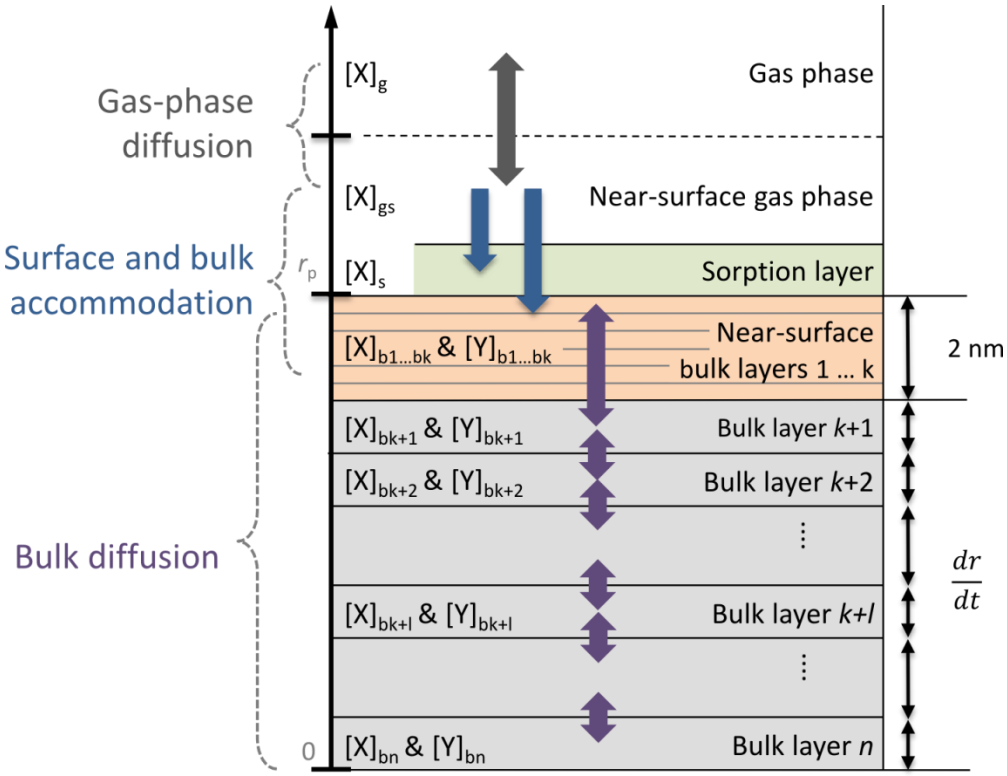


Figure S1. Schematic of KM-GAP and key mass transport processes including gas-phase diffusion (grey arrow), accommodation (blue arrow) and bulk diffusion (purple arrows). The near-surface bulk (orange box) has been resolved finely with *k* layers to keep track of a 1 nm surface region that is crucial for formation of an initial ice embryo in immersion freezing scenarios. All *n* bulk layers are allowed to grow and shrink.

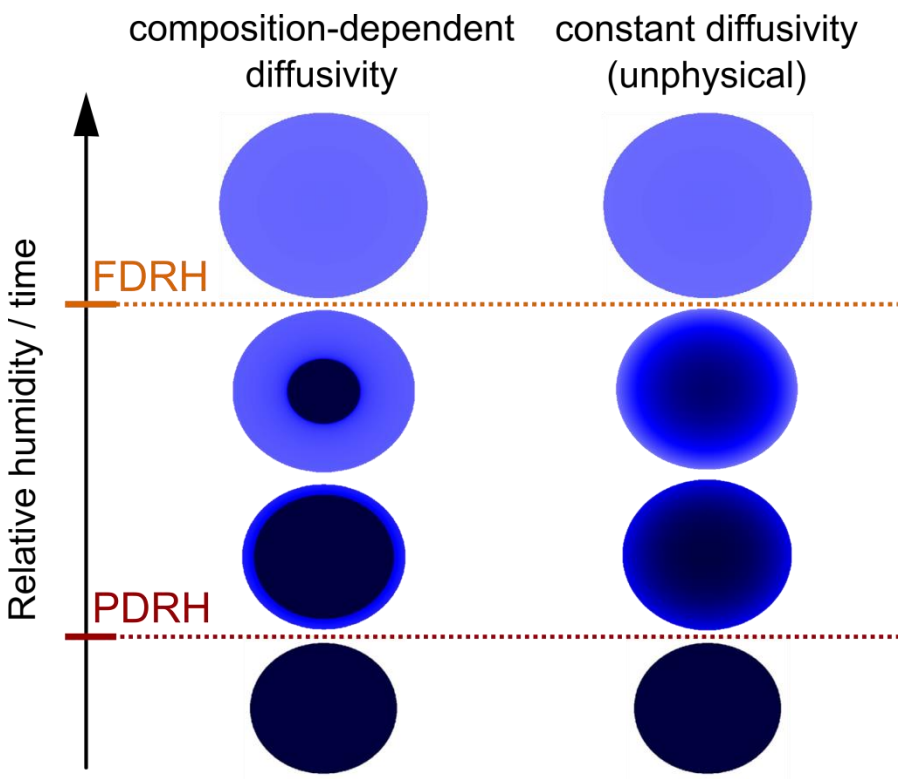


Figure S2. Schematic evolution of particle morphology upon humidification in two different scenarios. In the left column, diffusivity depends on water content and the liquefaction process is characterized by a sharp diffusion front moving into the particles. For comparison, the right column shows an unrealistic case of water diffusing into the particle with constant diffusivity.

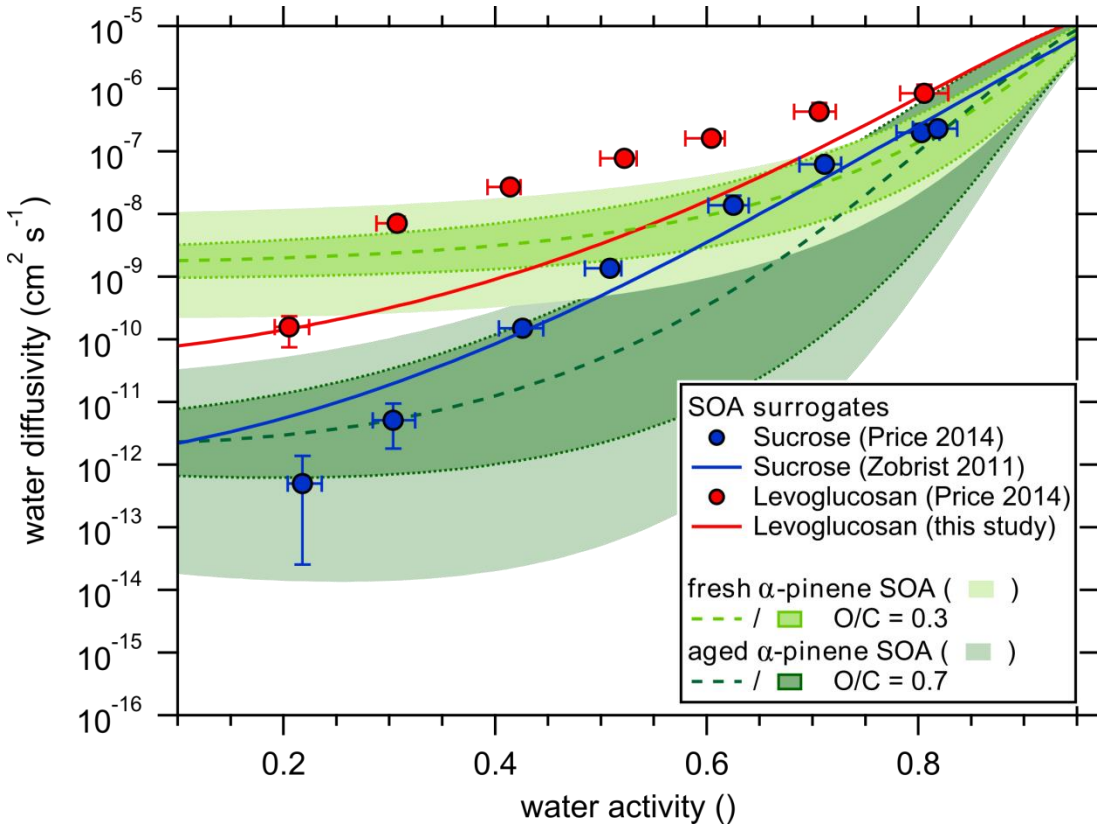


Figure S3. Estimated water diffusivity ranges for α-pinene SOA and comparison of water diffusivity in sucrose and levoglucosan matrices with experimental results by Price et al. (2014) at room temperature. DH2O in levoglucosan is higher than DH2O in sucrose, which is captured by the method proposed in this study. The differing curvature is a reminiscent feature of the sucrose parameterization used as a basis. Fresh α-pinene SOA (O/C = 0.3 ± 0.1, orange bands) shows higher DH2O than aged a-pinene SOA (O/C = 0.7 ± 0.1, green bands). The dark bands indicate uncertainty in DH2O at a fixed O/C (0.3 and 0.7, respectively) whereas the light bands indicate the entire expected range of DH2O in the given O/C range (0.2—0.4 and 0.6—0.8, respectively).

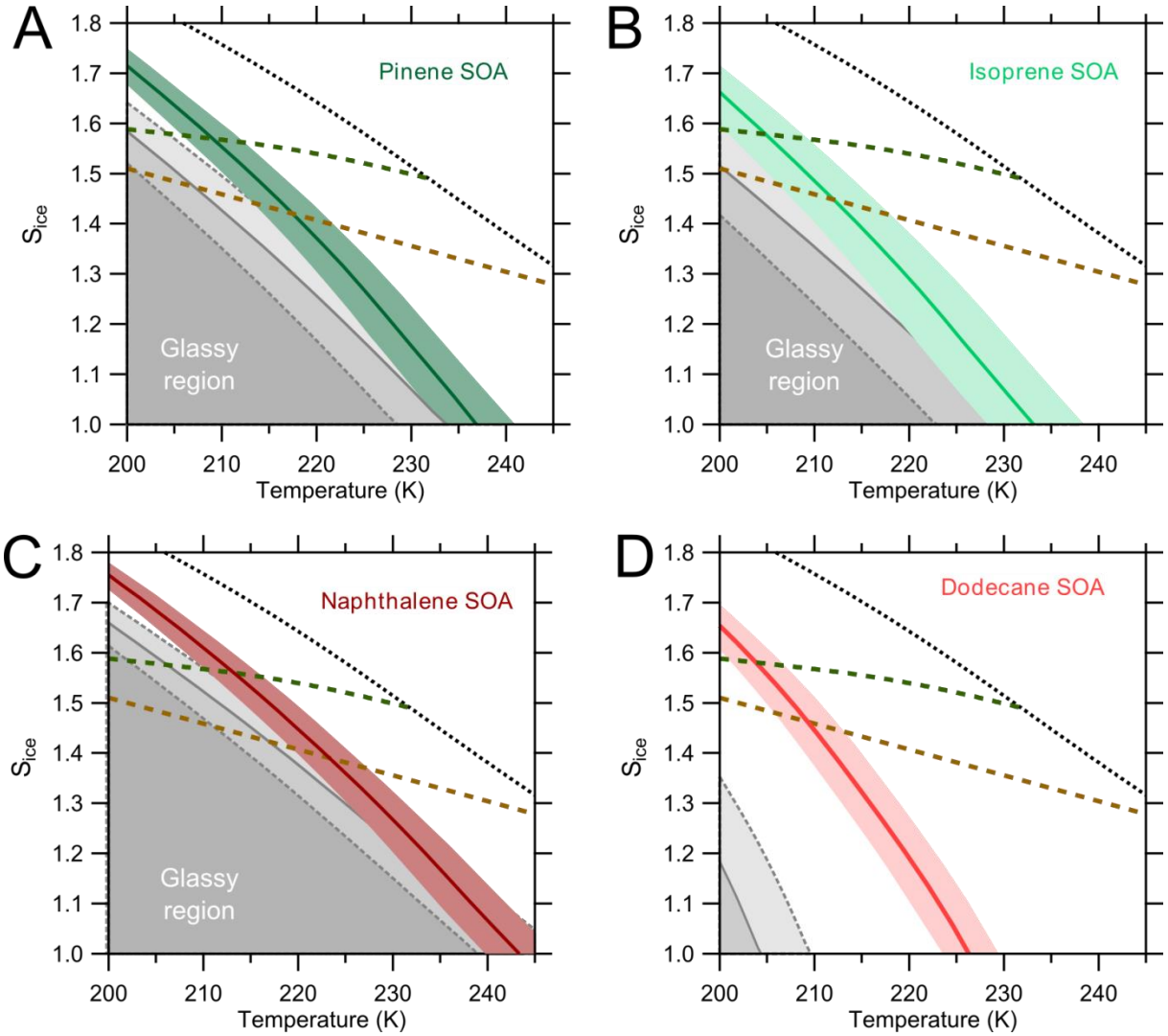


Figure S4. Quasi-equilibrium ($RH_g$, grey lines) and kinetic (FDRH, coloured lines) glass transition values of the four SOA precursor classes (A) a-pinene, (B) isoprene, (C) naphthalene, and (D) dodecane. Naphthalene SOA shows the highest glass transition values whereas dodecane SOA shows the lowest, in agreement with particle bounce experiments by Saukko et al. (2012). Uncertainty in quasi-equilibrium glass transition is given by dashed lines and grey shades; the uncertainty in FDRH is shown as shaded bands in the respective colour. These uncertainties arise from uncertainty in input parameters $\kappa_{org}$, $k_{GT}$ and $T_{g,org}$ as given in Table A1.

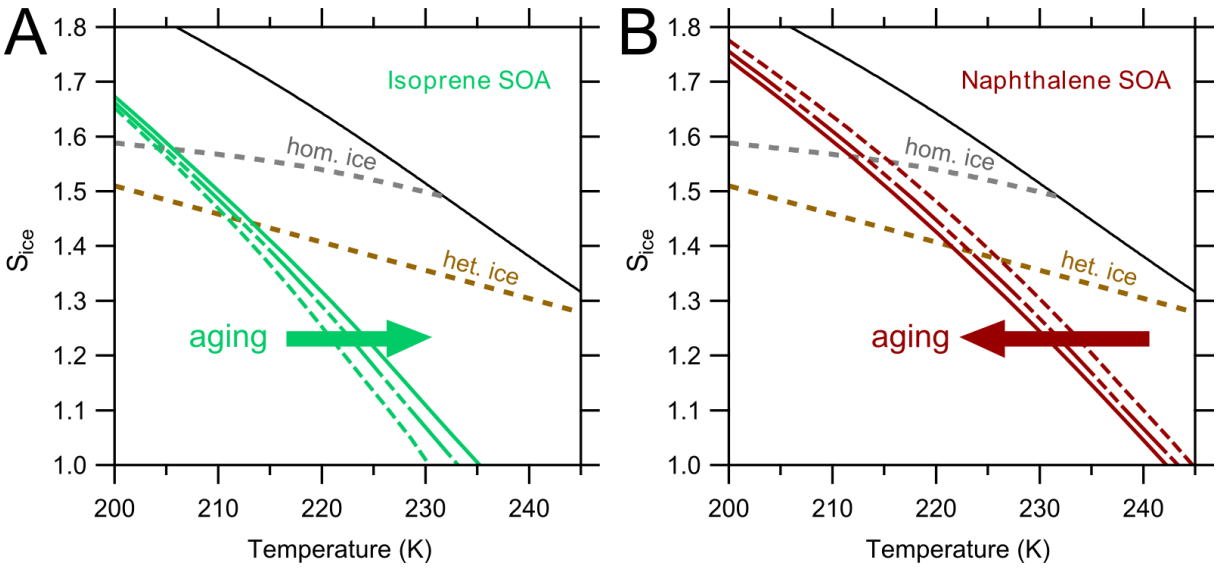


Figure S5. Effect of particle ageing on full deliquescence relative humidity (FDRH, solid and dashed lines) for (A) isoprene and (B) naphthalene SOA. Isoprene SOA shows slight hardening upon increase in O/C (indicated by higher FDRH), whereas Naphthalene SOA exhibits slight softening (indicated by lower FDRH).

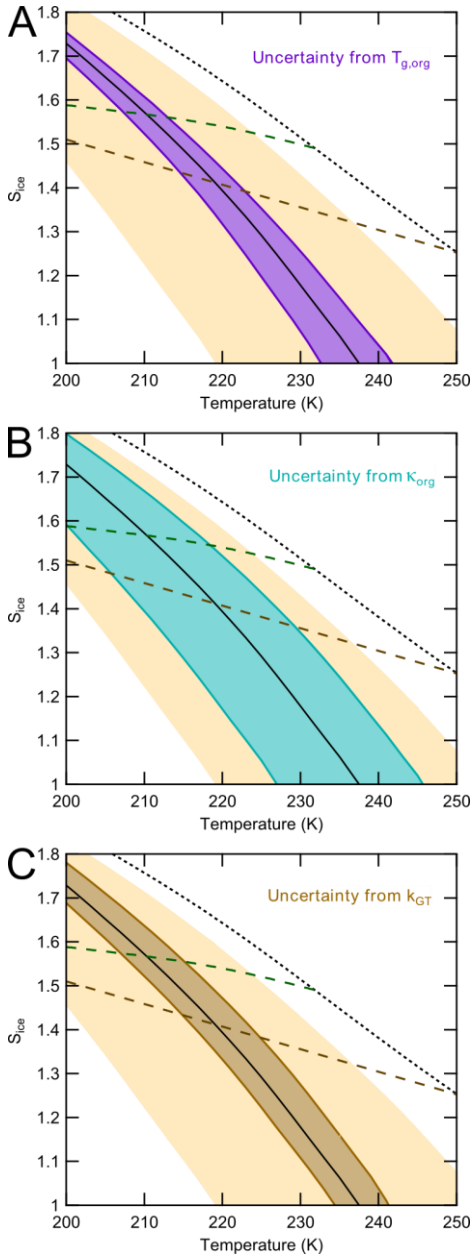


Figure S6. FDRH and uncertainties from different model input parameters in simulations of particle deliquescence (100 nm particles, humidified at a rate of 1 % RH $min^{-1}$, starting at $S_{ice}$ = 1) using the diffusivity estimation scheme along with the SOA best guess parameters of Koop et al. (2011) (cf. Table A1). The FDRH model results for the best guess parameters (black solid line) are subject to very high uncertainties when the full uncertainty range is considered, the orange shaded area denotes the worst possible scenario from the parameter ranges in Table A1. The uncertainty arising from sole uncertainty in $T_{g,org}$ is shown as purple shaded area in panel A, uncertainties arising from $\kappa_{org}$ and $k_{GT}$ are given in panels B and C and shaded in cyan and brown, respectively. Note that the displayed errors are not fully additive, i.e. the orange shaded area is not the sum of the purple, cyan and brown areas.

**Supporting Movies**

Movie S1. Simulation of humidification of a 200 nm sucrose particle from 60 % to 95 % RH at 215 K at a rate of 1 % RH $min^{-1}$. Water activity of the particle and ambient RH (left bottom corner) are colour-coded from dark blue (low $a_w$/RH) to light blue (high $a_w$/RH).

Movie S2. Simulated humidification of a 200 nm sucrose particle from 60 % to 95 % RH at 215 K under the unphysical assumption that water diffusivity does not change with water content and instead was fixed to $5 \cdot 10^{-14}$ $cm^2$ $s^{-1}$. The employed humidification rate is 1 % RH $min^{-1}$. Water activity of the particle and ambient RH (left bottom corner) are colour-coded from dark blue (low $a_w$/RH) to light blue (high $a_w$/RH).

## References


Angell, C. A.: in: Relaxations in Complex Systems, edited by: Ngai, K., and Wright, G. B., National Technical Information Service, I.S. Department of Commerce, Springfield, VA, 1985.

Angell, C. A.: Formation of glasses from liquids and biopolymers, Science, 267, 1924-1935, 1995.

Fulcher, G. S.: Analysis of recent measurements of the viscosity of glasses, J. Am. Ceram. Soc., 8, 339-355, 10.1111/j.1151-2916.1925.tb16731.x, 1925.

Gordon, M., and Taylor, J. S.: Ideal copolymers and the 2nd-order transitions of synthetic rubbers. 1. Non-crystalline copolymers, J. Appl. Chem., 2, 493-500, 1952.

Kautzman, K. E., Surratt, J. D., Chan, M. N., Chan, A. W. H., Hersey, S. P., Chhabra, P. S., Dalleska, N. F., Wennberg, P. O., Flagan, R. C., and Seinfeld, J. H.: Chemical Composition of Gas- and Aerosol-Phase Products from the Photooxidation of Naphthalene, J. Phys. Chem. A, 114, 913-934, 10.1021/jp908530s, 2010.

Kauzmann, W.: The nature of the glassy state and the behavior of liquids at low temperatures, Chem. Rev., 43, 219-256, 10.1021/cr60135a002, 1948.

Koop, T., Bookhold, J., Shiraiwa, M., and Pöschl, U.: Glass transition and phase state of organic compounds: dependency on molecular properties and implications for secondary organic aerosols in the atmosphere, Phys. Chem. Chem. Phys., 13, 19238-19255, 2011.

Lienhard, D. M., Bones, D. L., Zuend, A., Krieger, U. K., Reid, J. P., and Peter, T.: Measurements of Thermodynamic and Optical Properties of Selected Aqueous Organic and Organic-Inorganic Mixtures of Atmospheric Relevance, J. Phys. Chem. A, 116, 9954-9968, 10.1021/jp3055872, 2012.

Murphy, D. M., and Koop, T.: Review of the vapour pressures of ice and supercooled water for atmospheric applications, Q. J. R. Meteorol. Soc., 131, 1539-1565, 10.1256/qj.04.94, 2005.

Petters, M. D., and Kreidenweis, S. M.: A single parameter representation of hygroscopic growth and cloud condensation nucleus activity, Atmos. Chem. Phys., 7, 1961-1971, 2007.

Pöschl, U., Rudich, Y., and Ammann, M.: Kinetic model framework for aerosol and cloud surface chemistry and gas-particle interactions - Part 1: General equations, parameters, and terminology, Atmos. Chem. Phys., 7, 5989-6023, 2007.

Price, H. C., Murray, B. J., Mattsson, J., O'Sullivan, D., Wilson, T. W., Baustian, K. J., and Benning, L. G.: Quantifying water diffusion in high-viscosity and glassy aqueous solutions using a Raman isotope tracer method, Atmos. Chem. Phys., 14, 3817-3830, 10.5194/acp-14-3817-2014, 2014.

Saukko, E., Lambe, A. T., Massoli, P., Koop, T., Wright, J. P., Croasdale, D. R., Pedernera, D. A., Onasch, T. B., Laaksonen, A., Davidovits, P., Worsnop, D. R., and Virtanen, A.: Humidity-dependent phase state of SOA particles from biogenic and anthropogenic precursors, Atmos. Chem. Phys., 12, 7517-7529, 10.5194/acp-12-7517-2012, 2012.

Seinfeld, J. H., and Pandis, S. N.: Atmospheric chemistry and physics - From air pollution to climate change, John Wiley & Sons, Inc., New York, 2006.

Shiraiwa, M., Pfrang, C., Koop, T., and Pöschl, U.: Kinetic multi-layer model of gas-particle interactions in aerosols and clouds (KM-GAP): linking condensation, evaporation and

chemical reactions of organics, oxidants and water, Atmos. Chem. Phys., 12, 2777-2794, 10.5194/acp-12-2777-2012, 2012.

Stillinger, F. H.: Relaxation and flow mechanisms in fragile glass-forming liquids, J. Chem. Phys., 89, 6461-6469, 10.1063/1.455365, 1988.

Tammann, G., and Hesse, W.: The dependancy of viscosity on temperature in hypothermic liquids, Z. Anorg. Allg. Chem., 156, 14, 1926.

Vogel, H.: The temperature dependence law of the viscosity of fluids, Physik. Z., 22, 645-646, 1921.

Winkler, P. M., Vrtala, A., Rudolf, R., Wagner, P. E., Riipinen, I., Vesala, T., Lehtinen, K. E. J., Viisanen, Y., and Kulmala, M.: Condensation of water vapor: Experimental determination of mass and thermal accommodation coefficients, J. Geophys. Res. Atmos., 111, D19202, 10.1029/2006jd007194, 2006.

Yee, L. D., Craven, J. S., Loza, C. L., Schilling, K. A., Ng, N. L., Canagaratna, M. R., Ziemann, P. J., Flagan, R. C., and Seinfeld, J. H.: Secondary organic aerosol formation from low-$NO_x$ photooxidation of dodecane: evolution of multigeneration gas-phase chemistry and aerosol composition, J. Phys. Chem. A, 116, 6211-6230, 2012.

Zhang, X., Schwantes, R. H., Coggon, M. M., Loza, C. L., Schilling, K. A., Flagan, R. C., and Seinfeld, J. H.: Role of ozone in SOA formation from alkane photooxidation, Atmos. Chem. Phys., 14, 1733-1753, 10.5194/acp-14-1733-2014, 2014.

Zobrist, B., Marcolli, C., Pedernera, D. A., and Koop, T.: Do atmospheric aerosols form glasses?, Atmos. Chem. Phys., 8, 5221-5244, 2008.

Zobrist, B., Soonsin, V., Luo, B. P., Krieger, U. K., Marcolli, C., Peter, T., and Koop, T.: Ultra-slow water diffusion in aqueous sucrose glasses, Phys. Chem. Chem. Phys., 13, 3514-3526, 10.1039/c0cp01273d, 2011.

Zuend, A., and Seinfeld, J. H.: Modeling the gas-particle partitioning of secondary organic aerosol: the importance of liquid-liquid phase separation, Atmos. Chem. Phys., 12, 3857-3882, 10.5194/acp-12-3857-2012, 2012.